Effect of ZnS shell thickness on the phonon spectra in CdSe quantum dots

doi: 10.1103/PhysRevB.68.165306

Effect of ZnS shell thickness on the phonon spectra in CdSe quantum dots

A. V. Baranov
S.I. Vavilov State Optical Institute, St.-Petersburg, 199034, Russia

Yu. P. Rakovich* and J. F. Donegan
Physics Department, Trinity College, Dublin 2, Ireland

T. S. Perova and R. A. Moore
Department of Electronic and Electrical Engineering, Trinity College, Dublin 2, Ireland

D. V. Talapin
Institute of Physical Chemistry, University of Hamburg, 20146 Hamburg, Germany

A. L. Rogach
Department of Physics and CeNS, University of Munich, D-80799 Munich, Germany

Y. Masumoto
Institute of Physics, University of Tsukuba, Tsukuba 305-8501, Japan

I. Nabiev
EA n° 3306, IFR n° 53 "Biomolécules," Université de Reims Champagne-Ardene, 51, rue Cognacq Jay, 51100 Reims, France
(Received 27 June 2003; published 8 October 2003)

The evolution of the optical phonon spectra of colloidal core/shell CdSe/ZnS quantum dots with an increase of the shell thickness from 0.5 to 3.4 monolayers has been studied by resonant Raman spectroscopy. The results obtained suggest that the ZnS shell changes its structure from amorphous to partly crystalline as the thickness increases. Simultaneously, an increase in Raman scattering by surface (core/shell interface) phonons and the redshift of the corresponding phonon band have been observed and assigned to variations in the shell structure. The disorder present in the shell provides a major contribution to the line shape of the Raman spectra at higher ZnS coverage. A method to control the quality of quantum dots based on Raman spectroscopy is proposed.

DOI: 10.1103/PhysRevB.68.165306 PACS number(s): 78.30.Fs, 78.67.Bf, 78.68.+m, 68.35.Ja

I. INTRODUCTION

Highly luminescent II–VI semiconductor nanocrystals or colloidal quantum dots (QD's) have attracted much attention because of their applications in optoelectronics, nonlinear optics, and biology. It is known that the photoluminescence (PL) efficiency of QD's can be significantly improved by growing a shell of a wide-band-gap semiconductor around the QD core by analogy with two-dimensional semiconductor heterostructures.[1–3] A typical example is the CdSe/ZnS core/shell QD's possessing high PL quantum yield [$>50\%$ at room temperature (RT)].[3] In that case overcoating with ZnS results in the saturation of the CdSe dangling bonds, suggesting that surface native defects such as sulfur or cadmium vacancies can be efficiently eliminated by epitaxial growth of the shell. However, little is known about growth mechanism and the dependence of optical properties of nanocrystals on the shell parameters, e.g., the structure of the shell and the quality of the core/shell interface is not properly investigated yet. Whereas the internal structure of the core in the QD's can be studied by high-resolution transmission electron microscopy (HRTEM),[2,3] the internal structure of the shell and the interface between core and shell is not discernible due to lack of resolution. X-ray diffraction (XRD) analysis shows a clear contribution from the ZnS shell only for the samples with high ZnS coverage, because the scattering factors of ZnS are smaller than those of CdSe.[2]

In this paper, we explore Raman spectroscopy as a complementary tool to the HRTEM and XRD control of the shell structure in the core-shell CdSe/ZnS QD's. We proceed from the assumption that the surface (interface) modification during the shell growth must be accompanied by the changes in the phonon frequencies and line shape of Raman bands. The high sensitivity of Raman spectra to the surface reconstruction and contraction was demonstrated recently for CdSe nanocrystals capped with an organic ligand[4] and CdSe QD's embedded in glass or polymer matrices.[5–7] Here we present the results of optical phonon Raman studies of CdSe/ZnS QD's with different thickness of the ZnS shell which allows one to investigate the above-mentioned problem and make a conclusion concerning different growth regimes of ZnS shell.

II. EXPERIMENT AND CHARACTERIZATION OF SAMPLES

CdSe QD's capped with a shell of ZnS were prepared by an organometallic synthetic approach in a three-component

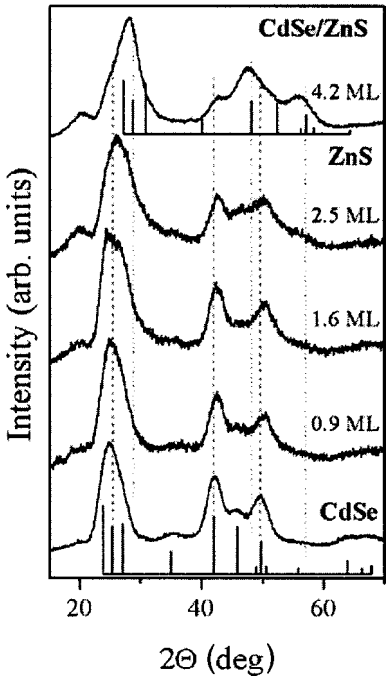

FIG. 1. Wide-angle powder x-ray diffractograms for 4.0-nm-diameter bare CdSe QD's and those overcoated by ZnS schell of different thickness (in monolayers, ML).

hexadecylamine–trioctylphosphine oxide–trioctylphosphine mixture.[3] Four samples with the same CdSe core size of 4.0 nm and the thicknesses of ZnS shell varying between ~0.5 monolayer (ML) and ~3.4 ML, together with the bare CdSe QD's of 4.0 nm size were used for spectroscopic measurements. Details of the chemical control of the core size and the shell thickness can be found elsewhere.[3]

The positions of the XRD peaks of the bare CdSe QD's match those of the bulk wurtzite CdSe, although the peaks are broadened because of the finite size of the QD's (Fig. 1). The peak structure remains almost the same for the low ZnS coverage (0.9 ML). Following further growth of the shell the XRD peaks become broader and the peak position shifts to higher diffraction angles, toward the position of the bulk ZnS wurtzite lines.

Absorption spectra of the colloidal solutions of QD's in toluene were measured using a Shimadzu UV-3101 PC spectrometer and the PL spectra were recorded using a Spex Fluorolog spectrometer equipped with a R943 Hamamatsu photomultiplier. The PL spectra were obtained by exciting the samples with a xenon lamp. The optical density of all samples was kept the same and below 0.2 at the first absorption feature for a 1-cm path length.

Figure 2 shows the evolution of optical properties of CdSe QD's in toluene for the thickness of the ZnS shell increasing from 0 to 3.4 ML. The absorption spectra shift to lower energies with increase of the shell thickness due to the partial tunneling of the electron wave function into the ZnS shell.[2] The well-pronounced absorption peaks at 2.3 eV and 2.7 eV are indicative for a narrow size distribution of CdSe/ZnS QD's, which was estimated to be 8% for the sample with a 0.5 ML thin ZnS shell. The PL spectra consist of a

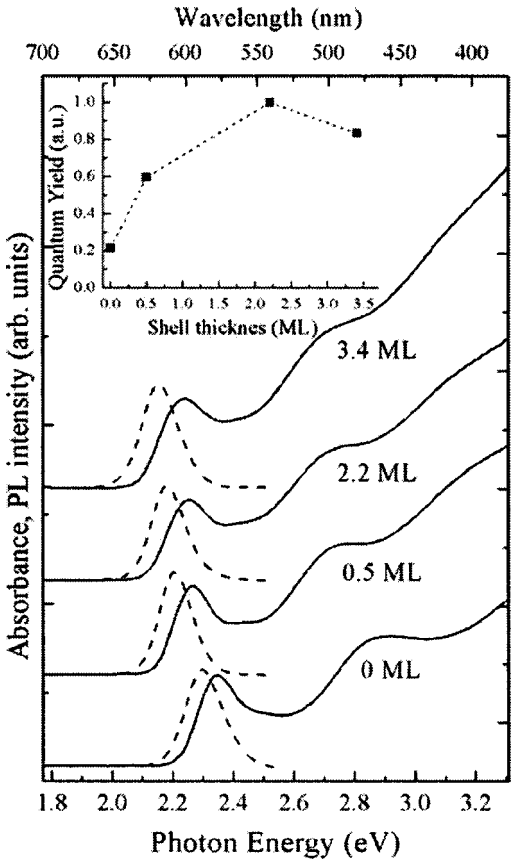

FIG. 2. Absorption (solid lines) and PL (dashed lines) spectra for the bare and ZnS coated CdSe QD's with different thickness of shell. Inset: The PL quantum yield as a function of the ZnS shell thickness. The dashed line is a guide to the eye.

sharp peak of the band-edge emission, indicating that the ZnS capping process greatly reduces the number of surface traps. Shifts in the PL peak position with increasing ZnS shell thickness are slightly larger than those in absorption. Both absorption and PL spectra show an increased broadening at higher ZnS coverage. This is most likely due to the increased size distribution (up to 12%) in the samples with thicker ZnS shell.[3] The inset in Fig. 2 shows an evolution of the PL quantum yield with increasing shell thickness. A significant improvement of the PL efficiency can be seen with increase of ZnS shell thickness up to 2.2 ML followed by a slight decrease in the quantum yield for the thickest coverage.

For the Raman measurements, QD's were deposited from their toluene solution on a Si wafer. The Raman spectra were excited by a 488 nm line of an Ar^+ laser with a power in the range 0.5–0.8 mW. The micro-Raman spectrometer (Renishaw-1000) equipped with 20× objectives and a cooled CCD camera was used in the experiments. Spectral resolution of the spectrometer was about 1 cm^{-1}. Each spectrum was averaged over 20 measurements with an accumulation time of 20 s. Because of the very high PL quantum efficiency of QD's (up to 55% at RT, as estimated by comparison with conventional laser dyes), resonant Raman spectra were usually superimposed on a broad luminescence background. This background has been subtracted in all

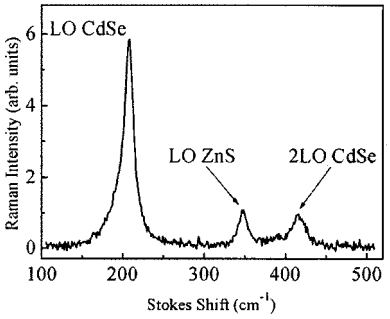

FIG. 3. Raman spectrum of CdSe/ZnS QD's with a shell thickness 3.4 ML excited by a 476.5-nm line of an Ar^{+2} laser.

spectra presented below in order to show more clearly the Raman signal itself. To detect weak Raman signals from the shell, 476.5-nm incident radiation has been used in combination with a highly sensitive spectrometer composed of a single monochromator equipped with a supernotch filter and a liquid-nitrogen cooled CCD detector. A spectral resolution of about 1.5 cm^{-1} was achieved in this case. All measurements were carried out at room temperature.

III. RESULTS

A. Electron-phonon coupling strength

As an example of the Raman spectra of the CdSe/ZnS nanocrystals, the spectrum of CdSe QD's with the thickest (3.4 ML) ZnS shell excited with 476.5-nm radiation is presented in Fig. 3. The Raman lines of the longitudinal optical (LO) and 2LO phonons of the CdSe core are clearly seen in the region of 200 cm^{-1} and 400 cm^{-1}, respectively. This multiphonon scattering is characteristic of the resonantly excited Raman processes in semiconductor QD's.[8] The electron-phonon coupling strength (S) can be roughly estimated from ratio between integrated intensities of the 2LO and LO lines.[9] We have obtain value of $S \approx 0.2$, which is the same order of magnitude as previously reported[8,10] for bare CdSe QD's and which is indicative of a much weaker electron-phonon coupling in CdSe/ZnS QD's than in the bulk CdSe ($S \sim 10$).[8]

B. ZnS phonon modes

We have also observed the line of the LO phonons of the ZnS shell at about 350 cm^{-1} (Ref. 11) with intensity comparable to that of 2LO CdSe peak (Figs. 3 and 4). This provides a report on the Raman response from the shell in CdSe/ZnS QD's. Assuming that the intensity and line shape of ZnS LO line is determined by shell crystallographic structure we have studied the Raman spectra in the region of the ZnS LO phonon for the shell thicknesses of 1 ML, 2.2 ML, and 3.4 ML [Figs. 4(a), 4(b), and 4(c), respectively]. The group of lines shown in Fig. 4 can be well fitted by three Lorentzians with variable amplitudes, peak positions, and full width at the half maximum (FWHM). It has turned out that the line of ZnS LO phonons at 350 cm^{-1}, which partly overlaps the second-order Raman lines of the CdSe core, can be distinguished, even at the shell thickness of 0.5 ML thick shell. The observed peak between ZnS LO and CdSe 2LO phonon lines can be assigned to the second-order Raman scattering by the surface optical (SO) phonon mode of CdSe.

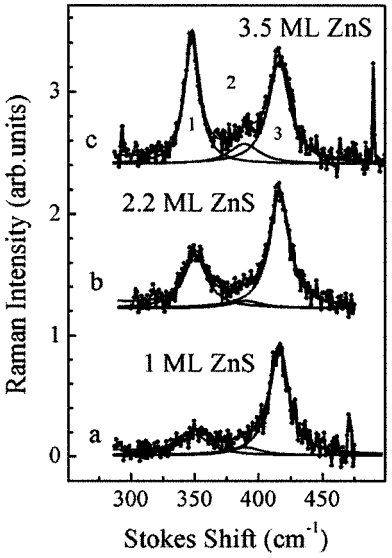

FIG. 4. The parts of the Raman spectra of CdSe/ZnS QD's in the region of the ZnS LO phonon for different shell thicknesses. The regions of the ZnS LO phonons and 2SO and 2LO phonons of CdSe are denoted by the numbers 1, 2, and 3, respectively. The solid curves are the result of the fitting procedure by the Lorentzian peaks. The excitation wavelength is 476.5 nm.

The dependencies of the ZnS LO phonon energy, Ω_{LO} (a), the FWHM of the related Raman line (b), and its integral intensity (c) on the ZnS shell thickness are presented in the Fig. 5. The ZnS LO line intensities of different samples were normalized to those of the CdSe 2LO line. Since the energy gap between the incident photon energy and the QD lowest energy absorption band increases progressively with ZnS thickness, a corresponding reduction of the CdSe 2LO line intensity would be expected. To take this effect into account the CdSe 2LO line intensities in the Raman spectra of different samples were first normalized by a factor

$$\frac{1}{(E_{EX}-E_{ABS})^2+\Delta E_{ABS}^2},$$

where E_{EX}, E_{ABS}, and ΔE_{ABS} are the incident photon energy ($\sim$2.61 eV), the peak energy, and the half width at half maximum (HWHM) (0.06 eV) of the lowest-energy QD absorption band. This factor describes the reduction of the resonant Raman intensity due to loss of resonance with a Lorentzian-type absorption band. Note, the effect is not important for qualitative conclusions because the values of the factor for samples with 0.5 ML and 3.5 ML ZnSe differ only in $\sim$1.18 times.

The increase in shell thickness results in the increase in the line integral intensity, which is roughly proportional to the ZnS volume. A remarkable decrease in linewidth from 30 cm^{-1} for the 0.5 ML shell down to 12.5 cm^{-1} for the 3.4 ML testifies to the substantial improvement in the shell crys-

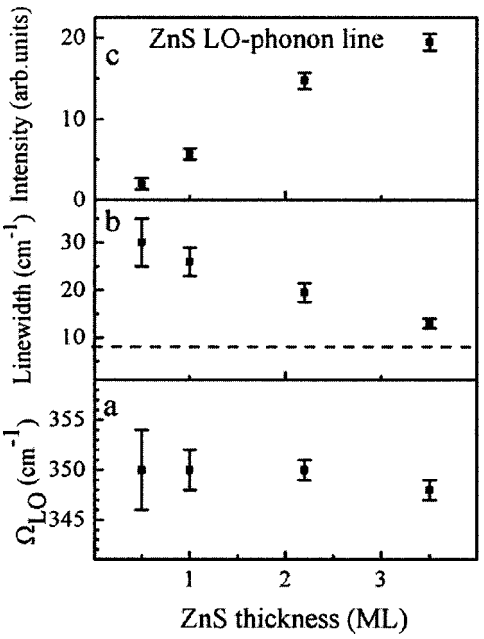

FIG. 5. The shell thickness dependence of the ZnS LO-phonon energy, Ω_{LO} (a), the FWHM of the related Raman line (b), and its integral intensity (c). A dashed line in (b) shows the FWHM of the LO-phonon line in a Raman spectrum of a high-quality bulk ZnS crystal (Ref. 11).

tallographic structure. At the same time an increase in the thickness of the ZnS shell does not lead to a noticeable shift of the LO band.

C. CdSe phonon modes

Let us now look more closely at the evolution of the first-order Raman spectra of the CdSe core as the ZnS shell thickness is varied. The Raman spectra of CdSe QD's covered by shells of different thickness are shown in Fig. 6, demonstrating an asymmetry of the Raman line shape in the low-frequency region. A good fit for the observed asymmetric spectra was obtained by taking the sum of two Lorentzian

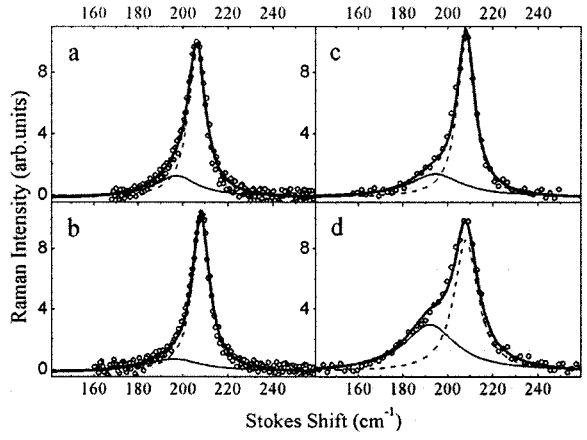

FIG. 6. The parts of the Raman spectra of CdSe/ZnS QDs in the region of the CdSe LO phonon for different shell thickness. The spectra were excited by a 488-nm line of an Ar^+ laser.

functions, which reveals a double structure in the Raman spectra. The more pronounced peak in each spectrum can be assigned to the Γ_1 LO phonon mode of CdSe. For the bare CdSe QD's the Stokes shift of the LO-phonon peak, Ω_{LO} of 206.1 cm^{-1}, is smaller than the corresponding bulk value of 210 cm^{-1} (Ref. 12) by 3.9 cm^{-1}. The shift originates from two sources: a redshift due to confinement of the optical phonons,[1] which is expected to be $\sim$4.7 cm^{-1} for 4-nm-large CdSe QD's and a blueshift caused by lattice contraction.[4] A 9.2-cm^{-1} width of the LO phonon line for the bare CdSe QD's in our experiment is in a close agreement with a value measured by a size-selective resonant Raman spectroscopy for a 4.2-nm-large CdSe QD's.[13]

IV. DISCUSSION

The origin of the low-energy "shoulder" of the CdSe LO peak was the subject of extensive discussion in the last several years.[6,7,13–15] In most of the studies it was suggested that the asymmetry in the low-frequency part of the LO-phonon Raman peak of CdSe QD's is caused mainly by the surface-optical (SO) phonon modes. In spite of the fact that the Raman scattering by the SO modes is forbidden for an ideal spherical shape of the QD's, the appearance of the SO peak in Raman spectra can be explained by the relaxation of the angular momentum phonon selection rule because of the lack of wave-vector conservation in QD's.[14] It has been also predicted that the SO mode can be observed in the Raman spectra in the case of nonspherical shape of the QD's, as well as due to the effect of impurities or interface imperfections.[13,14] A slightly elongated particle shape is known to be typical for colloidal CdSe QD's of the wurtzite phase, as evident from TEM and XRD results[2,5,16,17] and from the Rutherford backscattering spectroscopy.[18] Additional deviations from the spherical symmetry can be caused by a nonuniform growth of the ZnS shell.[2] Atomic displacement at the surface during growth (surface reconstruction) must also be taken ino account in the explanation of the observed features in the Raman spectra.[4,5] This surface induced structural disorder,[17,19] together with variations in thickness and shape of the ZnS shell and the presence of stacking faults,[2] can provide a major contribution to the line shape of the Raman spectra. Since the bare CdSe QD's can be considered as "free standing," the lattice reconstruction can be associated with surface tension and surface contraction.[17,19] Taking the above-mentioned factors into consideration we have analyzed the evolution of the LO-SO structure parameters with variation of the ZnS shell thickness.

The theory of the electron-phonon interaction shows that SO modes with $l \geqslant 1$, $m=0$ and those with $l=$even, $m=0$ can be involved into the Raman scattering via the deformation potential electron-phonon interaction[20,21] or the Fröhlich electron-phonon coupling,[14] respectively. Here l is the angular momentum and m is its projection. As only LO-phonon lines are observed in the spectra (Fig. 6) we believe that the polar interaction dominates the Raman process in our case. Thus we can assign the low-energy peak to the scattering from the SO phonon mode with $l=2$.

The energies of the SO modes, Ω_{SO}, are determined by

the energy of the TO phonons, Ω_{TO}, in CdSe QD's, the shape of the QD's,[14] and the dielectric constants of the core and surrounding medium. For spherical QD's they can be presented by the following equation:[21]

$$\Omega_{SO}=\Omega_{TO}\left[\frac{\varepsilon_0 l+\varepsilon_M(l+1)}{\varepsilon_\infty l+\varepsilon_M(l+1)}\right]^{1/2},$$

where ε_0 and ε_∞ are the static and high-frequency dielectric constants of the bulk CdSe and ε_M is the static dielectric constant of the surrounding medium. By assuming $\varepsilon_M=1$ (air) for the bare QD's and by using the bulk CdSe values of $\Omega_{TO}=167.5\ \mathrm{cm}^{-1}$, $\varepsilon_0=9.3$, $\varepsilon_\infty=6.1$,[12] we have calculated for the lowest ($l=2$) and the highest ($l\to\infty$) modes of spherical CdS QD's values of $\Omega_{SO}^{l=2}=199.7\ \mathrm{cm}^{-1}$ and $\Omega_{SO}^{l=\infty}=201.8\ \mathrm{cm}^{-1}$, respectively. The calculated $\Omega_{SO}^{l=2}$ energy is close to the experimental value obtained for the bare CdSe QD's ($\Omega_{SO}=197\ \mathrm{cm}^{-1}$). The difference of $2.7\ \mathrm{cm}^{-1}$, most likely, arises from a Ω_{SO} reduction due to the slightly ellipsoidal shape of the CdSe core.[14] The higher surface phonon modes ($l>2$) contribute only slightly to the scattering intensity between the SO and LO peaks, as can be seen from the good fit of the experimental line shape [Fig. 6(a)].

Figure 7 summarizes the ZnS thickness dependencies of the CdSe LO phonon energy, Ω_{LO} (a), the FWHM of the related Raman line (b), the SO mode energy (c), and the SO line FWHM (d) obtained as parameters of the fitting procedure. For the very thin ZnS shell of 0.5 ML, the LO band shifts to the high-energy side by $1.9\ \mathrm{cm}^{-1}$. It also becomes slightly narrower [Fig. 7(b)] and more symmetric [Fig. 6(a)]. We believe that for this shell thickness the amount of Zn and S atoms is not sufficient yet to create a complete ZnS layer. However, it is large enough to saturate in part the dangling orbitals of Cd and Se surface atoms, resulting in an increase in the PL quantum yield (Fig. 2, inset). It may be also possible that at this stage of shell formation, the core surface changes its morphology: the near-surface layer becomes more ordered. At the same time, the surface tension force becomes stronger resulting in the blueshift of the LO phonon energy induced by the CdSe lattice contraction, i.e., surface optimization[4] [Fig. 7(a)]. This surface reconstruction provides the minimum surface energy configuration and minimizes the surface state's contribution into PL efficiency (Fig. 2, inset). A further increase in the thickness of the shell up to 2.2 ML does not lead to a shift of the LO band or to the change in its width [Figs. 7(a), 7(b)]. The observed behavior supports the assumption that the reconstruction of the core surface stops at a ZnS thickness between 0.5 ML and 2.2 ML. Meanwhile the SO band continues to shift to lower energy ($194.5\ \mathrm{cm}^{-1}$) [Fig. 7(c)] and increases in intensity.

For a ZnS thickness of 3.4 ML, the SO phonon energy reduces even more [Fig. 7(c)] and the intensity of the SO-phonon line increases [Fig. 6(d)], while the LO-phonon band becomes broader [Fig. 7(b)]. Moreover, a slight disagreement can be seen between experimental and calculated line shapes in the spectral region between SO and LO peaks which is believed to be due to the enhanced scattering from all surface phonon modes with $l>2$ [Figs. 6(c), 6(d)].

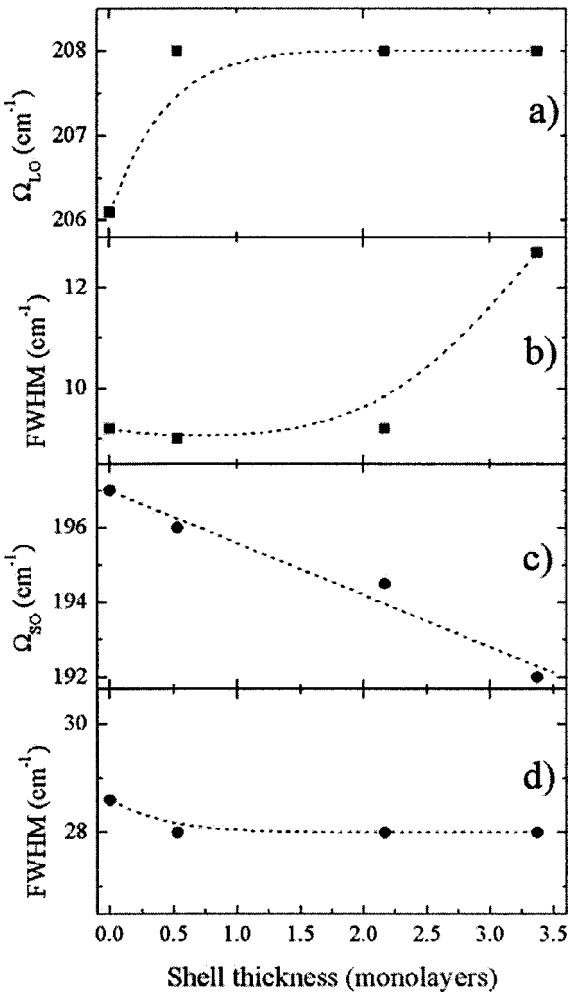

FIG. 7. The energies and linewidths of the LO (a), (b) and SO (c), (d) phonon modes in Raman spectra of the CdSe/ZnS QD's with different ZnSe shell thickness. The dashed lines are simply guides to the eye.

The observed changes of the Raman spectra can originate from the modification of the crystallographic structure of the ZnS shell and the reconstruction of the CdSe/ZnS interface which is associated with an increase in intensity and a decrease in energy of the SO mode with shell thickness. Indeed, the energy and intensity of the SO modes of the core/shell QD's depend on the value of the shell dielectric function (ε_M), which is in turn dependent on shell thickness. Of course, it is questionable if it is correct to describe an ultrathin ZnS layer by a macroscopic parameter ε_M. However, it is intuitively clear that the appearance and growth of the ZnS shell should be followed by increase of ε_M from its value corresponding to air up to some definite macroscopic value related to the bulk ZnS, resulting in modification of the SO mode parameters. In such a way, the decrease of Ω_{SO} with increasing shell thickness reflects the associated variation in the refractive index.

Note that the value of the SO-phonon frequency calculated using the dielectric constant of hexagonal ZnS, $\varepsilon_M=8.25$ (RT),[12] was about $182\ \mathrm{cm}^{-1}$. This differs from the measured Ω_{SO} of $192\ \mathrm{cm}^{-1}$. This fact leads to the assump-

tion that the ZnS shell is not ideally crystalline but is partly disordered, as has been concluded from analysis of the ZnS Raman spectra.

A remarkable decrease in the LO ZnS phonon linewidth with increase of the shell thickness [Fig. 5(b)] can suggest that the initially almost disordered shell structure gradually becomes crystalline. This conclusion is in agreement with results of the XRD studies of CdSe/ZnS QD's with variable shell thickness (Fig. 1). Indeed, increased broadening of the XRD peaks and observed shift of the peak position toward the position of the bulk ZnS lines provide evidence of a morphological transition from a disordered coherent interface to the incoherent epitaxial growth of the shell.[2,19]

From Fig. 1 we can roughly estimate the critical shell thickness to be about 2 ML when the crystal-like structure of the ZnS shell can be detected, although the increased broadening of the XRD peaks can be also attributed to the effect of crystalline defects such as stacking faults or twin boundaries and misfit dislocations.[2] As a result, the ZnS LO-phonon Raman linewidth of 12.5 cm^{-1} observed even for those QD's with the thickest shell, is still higher than that of the 7.9 cm^{-1} measured at room temperature for the LO-phonon Raman line in a high quality bulk ZnS crystal[11] [Fig. 5(b), dotted line]. It confirms that the structural disorder in the ZnS shell still exists at least at a shell thickness of 3.4 ML.

Crystallographic disorder in nanostructured materials is inevitable, and the presence of a disordered interfacial region, arising from incoherent shell growth, can induce amorphouslike features. The HRTEM measurements do not allow detection of a well-defined interface between the CdSe and the ZnS shell[3] and therefore some alloying can be expected in this region with content increasing with the shell thickness. It is well known that an increase in alloy content results in a decrease in the CdSe surface phonon frequencies[22] and can therefore explain the results presented in Fig. 6(c). However, we rule out the possibility of such modification of the interface as it would lead to a shift of the LO-phonon energy as well,[22] which was not observed in our case.

A significant broadening of the CdSe LO band at the ZnS thickness of 3.4 ML may suggest an effect of strain at the interface due to the 12% lattice mismatch between CdSe and ZnS. The formation of dislocations and grain boundaries should be associated with relaxation of the crystallographic structure and creation of sources for nonradiative recombination sites in the ZnS shell.[2] The interfaces can also contain random irregularities in shape. Even though ZnS capping saturates dangling bonds and reduces the number of surface defects, the latter may be replaced with interface imperfections. It is significant that the quantum yield in our samples decreases at higher surface coverage (Fig. 2, inset). This behavior lends support to the suggestion for generation of structural defects. On the other hand, the absence of a spectral shift of the LO-phonon band implies that the core surface is already relaxed and probably defect-free. Thus our results provide a further support for an incoherent epitaxial mechanism for the growth of the ZnS shell at high coverage, as was suggested in Ref. 2. When the structure of the shell is well established, the phonons confined in the core may collide and relax at the interface and contribute to the broadening of the phonon lines. Therefore we believe that the observed broadening of the LO-phonon band mainly originates from the shell-induced disorder.

In conclusion, we have shown the influence of ZnS shell thickness on the Raman scattering intensities, energies, and broadening of optical phonons in the CdSe/ZnS core/shell QD's. The analysis of Raman spectra in combination with XRD, PL, and absorption spectroscopy results suggests that a morphological transition from semidisordered coherent (at very low coverage) to the incoherent epitaxial (at shell thickness more that 2 ML) takes place in the growth mechanism of the ZnS shell on the CdSe core. As a result, a defect-free core/shell interface is more important for producing strongly luminescent QD's than an increase of the shell thickness. We suggest that the independence of the CdSe LO phonon energy on shell thickness as well as the significant broadening of the CdSe LO line, observed at high coverage, can be used as a tool to control the shell thickness in order to provide the highest quality QD's.

ACKNOWLEDGMENTS

The work was supported in part by the Enterprise Ireland International Collaboration Program (Grant No. IC/2002/071) and the Science Foundation Ireland (Grant No. 02/IN.1/I47). A.V.B. acknowledges INTAS (Grant No. 01-2331) and JSPS (Grant No. S-02218) for partial financial support.

*Corresponding author. Electronic address: Yury.Rakovich@tcd.ie

[1] M.A. Hines and P. Guyot-Sionnest, J. Phys. Chem. **110**, 468 (1996).

[2] B.O. Dabbousi, J. Rodriguez-Viejo, F.V. Mikulec, J.R. Heine, H. Mattoussi, R. Ober, K.F. Jensen, and M.G. Bawendi, J. Phys. Chem. **101**, 9463 (1997).

[3] D.V. Talapin, A.L. Rogach, A. Kornowski, M. Haase, and H. Weller, Nano Lett. **1**, 207 (2001).

[4] J.-Yu. Zhang, X.-Y. Wang, M. Xiao, L. Qu, and X. Peng, Appl. Phys. Lett. **81**, 2076 (2002).

[5] J.J. Shiang, A.V. Kadavanich, R.K. Grubbs, and A.P. Alivisatos, J. Phys. Chem. **99**, 17417 (1995).

[6] Y.-N. Hwang, S. Shin, H.L. Park, S.-H. Park, U. Kim, H.S. Jeong, E.-J. Shin, and D. Kim, Phys. Rev. B **54**, 15120 (1996).

[7] Y.-N. Hwang, S.-H. Park, and D. Kim, Phys. Rev. B **59**, 7285 (1999).

[8] M.C. Klein, F. Hache, D. Ricard, and C. Flytzanis, Phys. Rev. B **42**, 11123 (1990).

[9] A.P. Alivisatos, T.D. Harris, P.J. Carroll, M.L. Steigerwald, and L.E. Brus, J. Chem. Phys. **90**, 3463 (1989).

[10] A.P. Alivisatos, A.L. Harris, N.J. Levinos, M.L. Steigerwald, and L.E. Harris, J. Chem. Phys. **89**, 4001 (1988).

[11] M. Siakavellas, A.G. Kontos, and E. Anastassakis, J. Appl. Phys. **84**, 517 (1998).

[12] *Semiconductors*, edited by O. Madelung, W. von der Osten, and U. Rössler (Springer, Berlin, 1982), Landolt-Burstein, New Series, Group III, Vol. 22a.

[13] C. Trallero-Giner, A. Debernardi, M. Cordona, E. Menendez-

Proupin, and A.I. Ekimov, Phys. Rev. B **57**, 4664 (1998).
[14] F. Comas, C. Trallero-Giner, N. Studart, and G.E. Marques, Phys. Rev. B **65**, 073303 (2202).
[15] R. Rodriguez-Suarez, E. Menendez-Proupin, C. Trallero-Giner, and M. Cardona, Phys. Rev. B **62**, 11006 (2000).
[16] C.B. Murray, D.J. Norris, and M.G. Bawendi, J. Am. Chem. Soc. **115**, 8706 (1993).
[17] K.S. Hamad, R. Roth, J. Rockenberger, T. van Buuren, and A.P. Alivisatos, Phys. Rev. Lett. **83**, 3474 (1999).
[18] J. Taylor, T. Kippeny, S.J. Rosenthal, J. Cluster Sci. **12**, 571 (2001).
[19] M.G. Bawendi, A.R. Kortan, M.L. Steigerwald, and L.E. Brus, J. Chem. Phys. **91**, 7282 (1989).
[20] R. Ruppin, R. Englman, Rep. Prog. Phys. **33**, 146 (1970).
[21] A.V. Fedorov, A.V. Baranov, K. Inoue, Phys. Rev. B **56**, 7491 (1997).
[22] A. Mlayah, A.M. Brugman, R. Carles, J.B. Renucci, M.Ya. Valakh, A.V. Pogorelov, Solid State Commun. **90**, 567 (1994).